CHEMISTRY OF MATERIALS

Article

pubs.acs.org/cm

Electronic Properties of Transparent Conductive Films of PEDOT:PSS on Stretchable Substrates

Darren J. Lipomi,[†] Jennifer A. Lee,[†] Michael Vosgueritchian,[†] Benjamin C.-K. Tee,[‡] John A. Bolander,[‡] and Zhenan Bao[†,*]

[†]Department of Chemical Engineering and [‡]Department of Electrical Engineering, Stanford University, Stanford, California 94305, United States

Supporting Information

ABSTRACT: Despite the ubiquity of poly(3,4-ethylenedioxythiophene):poly(styrenesulfonate) (PEDOT:PSS) as a transparent conducting electrode in flexible organic electronic devices, its potential as a stretchable conductor has not been fully explored. This paper describes the electronic and morphological characteristics of PEDOT:PSS on stretchable poly(dimethylsiloxane) (PDMS) substrates. The evolution of resistance with strain depends dramatically on the methods used to coat the hydrophobic surface of PDMS with PEDOT:PSS, which is cast from an aqueous suspension. Treatment of the PDMS with an oxygen plasma produces a brittle skin that causes the PEDOT:PSS film to fracture and an increase in resistivity by four orders of magnitude at only 10% strain. In contrast, a mild treatment of the PDMS surface with ultraviolet/ozone (UV/O_3) and the addition of 1% Zonyl fluorosurfactant to the PEDOT:PSS solution produces a mechanically resilient film whose resistance increases by a factor of only two at 50% strain and retains significant conductivity up to 188% strain. Examination of the strained surfaces of these resilient PEDOT:PSS films suggests alignment of the grains in the direction of strain. Wave-like buckles that form after the first stretch >10% render the film reversibly stretchable. Significant cracking (~2 cracks mm^{-1}) occurs at 30% uniaxial strain, beyond which the films are not reversibly stretchable. Cyclic loading (up to 1000 stretches) produces an increase in resistivity whose net increase in resistance increases with the value of the peak strain. As an application, these stretchable, conductive films are used as electrodes in transparent, capacitive pressure sensors for mechanically compliant optoelectronic devices.

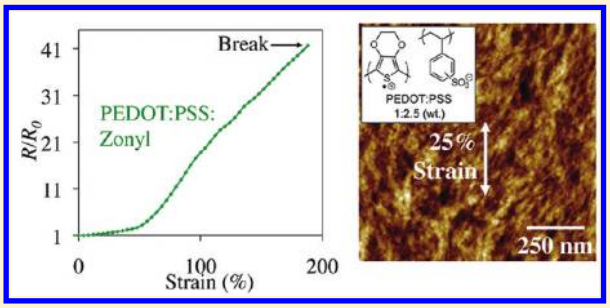

KEYWORDS: *stretchable electronics, stretchable solar cells, PEDOT:PSS, Zonyl, PDMS*

INTRODUCTION

Materials that combine optical, electronic, and mechanical properties are scientifically interesting as well as technologically useful.[1] For example, thin films that exhibit transparency, conductivity, and elasticity under tensile strain could enable applications in off-grid solar energy harvesting[2] and storage,[3] devices for biomedicine[4,5] and artificial intelligence,[6,7] and collapsible, rugged consumer electronics such as displays.[8] Ideally, the stretchable, transparent electrode would be smooth and homogeneous and could extract or inject charge anywhere on its surface (e.g., from or to organic semiconductors) without the need for charge transporting layers, as are needed in, for example, films of metallic nanowires.[9]

This paper describes the behavior of thin films of poly(3,4-ethylenedioxythiophene):poly(styrene sulfonate) (PEDOT:PSS, Figure 1), mixed with Zonyl fluorosurfactant,[10] on poly(dimethylsiloxane) (PDMS) substrates as stretchable transparent electrodes. Despite the ubiquity of PEDOT:PSS as a transparent conductor in mechanically compliant organic electronic devices, the behavior of the material under significant (>10%) tensile strains on compliant substrates has not been fully characterized. We found—using the conditions described in this paper—that films of PEDOT:PSS retain significant conductivity up to 188% strain and are reversibly stretchable up to 30% strain. We investigated the effects of different methods of activating the surface of PDMS on the electromechanical properties of the films. We found that treatment with an oxygen

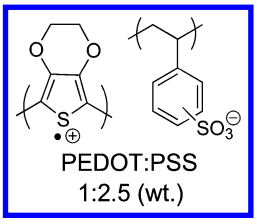

Figure 1. Chemical structures of the components of PEDOT and PSS. There is approximately one positive charge for every three EDOT monomers. The formulation sold as Clevios PH1000 is a 1:2.5 mixture of PEDOT and PSS.

Received: October 26, 2011
Revised: December 20, 2011
Published: December 22, 2011

plasma produced a brittle surface that rendered the PEDOT:PSS film susceptible to fracture: the resistance increased 4 orders of magnitude with 10% strain. Treatment of the surface with ultraviolet/ozone (UV/O_3) maintained the elasticity of the bulk PDMS. On these surfaces, the resistance of PEDOT:PSS films increased by a factor of only 2 with 50% strain. These findings have implications for electronic devices that require significant mechanical compliance.

Stretchable Conductors. Stretchable electronics is an extension of flexible electronics.[11] While devices that offer flexibility can be produced by roll-to-roll manufacturing[12] and are collapsible, many of the most interesting and important applications of thin-film electronic devices in the future will require stretchability.[1] Integration of electronics with moving parts, conformal bonding of electronics to nonplanar substrates, and resistance of devices to mechanical failure require significant elasticity in response to tensile strains (ε).[13−15] Ordinary electronic materials exhibit poor tolerance to tensile strain: crystalline silicon fractures at ∼0.7% strain,[16] and the best organic semiconductors are often brittle.[17,18] The goal of stretchable electronics is to produce materials that can undergo large strains (e.g., $\varepsilon \geq 10\%$) without cracking. For applications requiring one-time stretchability (e.g., to bond to nonplanar surfaces) the strain need not be reversible. For applications requiring repeated deformation and resistance to fracture, however, tensile elasticity—not just stretchability—is required.

There are now several types of elastic, stretchable composite conductors in the literature that rely on forming percolated networks of conductive particles (e.g., carbon nanotubes[14] and metallic particles[19]) in elastic matrices. These composite materials are, however, not intended to be transparent. Stretchable thin-film electrodes include fractured metallic films that form percolated pathways in the stretched state, as demonstrated by Wagner,[20] Lacour,[21] and co-workers. Stec et al. recently described ultrathin films of gold[22] that could perhaps be rendered stretchable by controlled fracture. Networks of copper[23] and silver[24] nanowires prepared by solution-phase synthesis or electrospinning[9] have demonstrated stretchability or flexibility (which implies stretchability to an extent that depends on the thickness of the substrate and the radius of bending[25]). Films of carbon nanotubes[26] and graphene[27] on elastomeric substrates can be reversibly stretchable. In a previous report from our laboratory, we described transparent films of single-walled carbon nanotubes that were reversibly stretchable up to 150% along two axes.[28] In a related example, Yu et al. described an elastic thin film comprising nanotubes and an elastomer, which the authors used as an electrode for stretchable organic light-emitting devices.[29] A challenge associated with all films that rely on percolated pathways is that they can only extract and inject charge near the individual particles—e.g., nanowires—that make up the conductive network.

PEDOT:PSS. Poly(3,4-ethylenedioxythiophene):poly(styrenesulfonate) is an intrinsically conductive polyelectrolyte complex; it has been sold commercially for two decades and is used as an antistatic coating for photographic film.[30] Its ubiquity as a transparent electrode material in organic optoelectronic devices has made it the subject of several hundred publications per year: the monograph by Elschner et al. is a thorough review of this work as of 2010.[30] The polymerization of EDOT is catalyzed by Fe(III) in the presence of excess peroxydisulfate, which also oxidizes ("dopes") the resulting polymer to render it conductive. Polymerization in a solution containing excess PSS—a polyanion that balances the positively charged PEDOT backbone—renders the complex soluble in water.[30] There is approximately one positive charge per three EDOT monomers. PEDOT:PSS is sold commercially by Heraeus under the trade name Clevios, a family of formulations which differ primarily on the basis of the ratio of PEDOT to PSS; in general, the conductivity increases with this ratio. We used the formulation Clevios PH1000 for this work, which has a ratio of 1:2.5 by weight and an advertised conductivity of 1000 S cm^{-1}.

Achieving the maximum conductivity requires a "secondary dopant," which is typically a polar, high-boiling solvent. The standard secondary dopant is dimethylsulfoxide (DMSO), added at a concentration of 5% (the amount used for all of the experiments in this paper). When added to the solution before casting, the high-boiling solvent allows the PEDOT to form large, interconnected grains on the scale of ∼10 nm.[31] Previous work from our laboratory has demonstrated that Zonyl fluorosurfactant (FS-300), an amphiphilic material whose molecular structure consists of a hydrophilic poly(ethylene oxide) head and a hydrophobic poly(tetrafluoroethylene) tail, also has the effect of a secondary dopant for PEDOT:PSS.[10] The addition of Zonyl to the solution used for spin-coating, further, permits coating of hydrophobic substrates.[10]

Mechanical Properties of PEDOT:PSS. PEDOT:PSS can exhibit values of transparency and conductivity close to those of tin-doped indium oxide (ITO)[32] but is more mechanically compliant than ITO.[33] The Young's modulus of PEDOT:PSS is approximately 2 GPa,[18] as determined by the buckling method.[34] This value is close to that of both PEDOT and PSS; thus, the stiffness is not expected to be a strong function of the ratio of the components.[18] PEDOT:PSS has been used as a conductor in many unconventional, mechanically compliant applications. For example, Invernale et al. soaked Spandex and other fabrics in PEDOT:PSS for stretchable electrochromic textiles that could be stretched up to 100%.[35,36] Blau et al. described all-polymer microelectrode arrays for cardiac and neuronal electrophysiology incorporating PEDOT:PSS.[37] Hansen et al. has prepared an inkjet-printable composite material by polymerizing poly(3,4-ethylenedioxythiophene) in a complex with *para*-toluenesulfonate in solution with polyurethane.[38] The conductive elastomer exhibited a conductivity of 100 S cm^{-1} at 100% strain and was reversibly stretchable up to 50% strain; however, it remained conductive up to 200%.[39] The films were thick (500−700 nm), however, and it is likely that the presence of the insulating polyurethane limits the maximum achievable conductivity. Kwon et al. described a complex of PEDOT and a polyionic liquid that could tolerate extremely high strains (350%) with only twofold increase in resistance, but the material exhibited low initial conductivity of 10^{-3} S cm^{-1}.[40]

In a previous report, we described the use of buckled films of PEDOT:PSS on elastic substrates as the stretchable, hole-conducting electrodes in stretchable organic solar cells.[41] The films were rendered stretchable by spin-coating on prestrained PDMS membranes. At a thickness of 100 nm, these films had sheet resistances of 750 Ω/sq at 95% transparency and could be stretched to the value of the prestrain.[41] We used the buckling strategy because a planar film of the brittle organic semiconducting active layer cracked upon the application of strain. The goal of the present work was to generate conductive films that were stretchable, reversibly, without prestraining the substrate. We reasoned that commercial PEDOT:PSS, which

dx.doi.org/10.1021/cm203216m | *Chem. Mater.* 2012, 24, 373−382

already possesses an excellent combination of sheet resistance and transparency when doped with 5% dimethylsulfoxide,[32] could be rendered stretchable if supported by an unprestrained PDMS membrane, given the right additives and treatment of the PDMS.

Requirements of Stretchability. For flexible applications, a transparent conductive film of thickness d_f must, at minimum, accommodate the peak strain (ε_{peak}) associated with the smallest bending radius (r) the device will experience during normal use. The peak strain is directly related to the thickness of the substrate (d_s) by eq 1.[25]

$$\varepsilon_{peak} = \left(\frac{d_f + d_s}{2r}\right) \times 100\% \quad (1)$$

Bending a film (for which $d_f \ll d_s$) on a flexible substrate with 100-μm thickness to a radius of 5 mm thus produces a peak strain of 1%.[16] Placing the stiffest components of a device in the neutral mechanical plane—where the compressive and tensile strains produced by bending are counterbalanced—can decrease the risk of mechanical failure.[25,42] Increasing the failure strain of electronic materials could further increase the lifetime of devices (particularly those intended for fieldwork[8]) and enable applications in stretchable electronics.

RESULTS AND DISCUSSION

Deposition of PEDOT:PSS Films on PDMS. The low native surface energy of PDMS (water contact angle = 112°) precluded spin-coating of PEDOT:PSS, which is usually coated from an aqueous suspension. We explored three methods for activating the surface of PDMS: (1) oxidation by exposure to ultraviolet/ozone (UV/O_3, contact angle = 90°); (2) oxidation with an oxygen plasma ("plasma", water contact angle < 5°); and (3) hydrolysis of the surface with 10% hydrochloric acid ("HCl", contact angle = 91°). The ability to form films was facilitated by adding Zonyl to the PEDOT:PSS solution in a concentration of 1%.[10,43] A minimum exposure of 20 min of UV/O_3 was required to form a film of PEDOT:PSS with 1% Zonyl, while a minimum exposure of 10 s of an oxygen plasma at 150 W and 400 mtorr O_2 was required to form a film of PEDOT:PSS with 0% Zonyl. We were unable to form films of PEDOT:PSS without Zonyl on PDMS substrates treated with UV/O_3 for ≤ 60 min. All films were spin-coated at the same speed (1 krpm for 60 s and then 2 krpm for 60 s), which produced films with thicknesses of 70 nm. The sheet resistance and transparency of the films spin-coated from solution containing 5% DMSO and 1% Zonyl were 260 Ω/sq at 95% transparency. The bulk conductivity (σ) was 550 S cm^{-1}. Films spin-coated on glass substrates activated using an oxygen plasma had the same sheet resistance as those spin-coated on PDMS activated with UV/O_3.

Evolution of Resistance with Strain. We measured resistance versus strain for a PEDOT:PSS film spin-coated from a solution containing 1% Zonyl on a PDMS substrate activated using UV/O_3. Figure 2a plots the normalized resistance of the film when stretched from 0% to 200% strain. The resistance increased in two phases. In the first phase, from 0% to 50% strain, the increase in resistance was relatively small, and the resistance at 50% strain was 2.7 times its initial value. From 50% strain to 188% strain (at which the PDMS substrate failed), the resistance was 42 times its initial value. A bare PDMS substrate treated with UV/O_3 exhibited neither buckling nor cracking after one full cycle of stretching and relaxation to

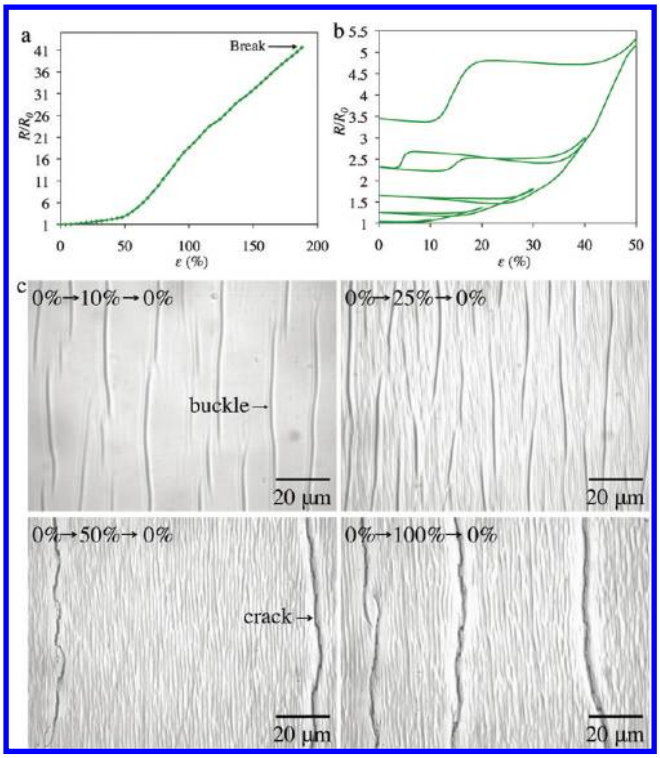

Figure 2. Evolution of normalized resistance (R/R_0) and morphology vs strain (ε) for films of PEDOT:PSS on UV/O_3-treated PDMS. (a) Normalized resistance of a film when stretched from 0% to 200%. The PDMS substrate fractured at 188% strain. (b) Normalized resistance vs strain for a film that underwent incremental stretching from 0% → 10% → 0% → 20% → 0% → 30% → 0% → 40% → 0% → 50% → 0%. (c) Optical microscope images of PEDOT:PSS films on PDMS after stretching and releasing the films from strains of 10%, 25%, 50%, and 100% along the horizontal axis. Buckles appear after stretching ≥10%, while significant cracking (>2 cracks mm^{-1}) occurs at strains >30%. At 50% strain, the frequency of cracks is 60 mm^{-1}. Upon straining to 100%, the frequency is 140 mm^{-1}.

150% strain. Figure 2b shows the evolution of resistance versus strain for a film that underwent five cycles of loading with progressively greater strains: 0% → 10% → 0% → 20% → 0% → 30% → 0% → 40% → 0% → 50% → 0%. The resistance is a strong function of its strain history. For the first three intervals over which the film is unloaded (i.e., 10% → 0%, 20% → 0%, and 30% → 0%), the plot is relatively flat. When the film is subsequently stretched (e.g., to 20%, 30%, and 40%), the data nearly overlap with those produced during the previous unloading. When the film is stretched beyond the previous maximum strain (e.g., when the film is stretched past 20% on the way to 30%), the resistance increases, irreversibly. The dependence of resistance on strain is reversible for strains ≤ 30%. We will return to the topic of reversibility and cyclic loading.

Films of PEDOT:PSS on UV/O_3-treated substrates appeared to have three regimes by which they accommodated strain: elastic deformation, plastic deformation, and brittle fracture. Figure 2c shows optical micrographs of four samples of the same PEDOT:PSS film after stretching to and releasing from strains of 10%, 25%, 50%, and 100%. Straining and releasing the substrate to <10% produced no features in the PEDOT:PSS films that were visible by optical microscopy. After stretching the PEDOT:PSS/PDMS substrates to and releasing them from a strain of ≥10%, the PEDOT:PSS films exhibited nonperiodic

dx.doi.org/10.1021/cm203216m | Chem. Mater. 2012, 24, 373–382

buckles of the type visible in Figure 2c (top left). These raised features in the film appear to be locally delaminated from the PDMS surface; we did not, however, observe any instance in which the film pulled away from the edges of the substrate, which would imply global delamination and slipping of the film against the PDMS substrate. The sample stretched to and released from 25% exhibited regular, periodic buckling, and some cracking. The film stretched to 50% exhibited cracks with a frequency of 60 cracks mm^{-1}, and the film stretched to 100% exhibited cracks with a frequency of 140 cracks mm^{-1}. The frequency of buckling (260 buckles mm^{-1}) was approximately the same for the films stretched and released from 50% and 100% strain. The observation of buckling after straining ≥10% was probably a manifestation of irreversible (plastic) deformation of the PEDOT:PSS film. Subsequent relaxation of the PDMS substrate compressed the permanently elongated PEDOT:PSS film, and the buckles in the film formed to accommodate the compressive strain.

In a separate experiment, we stretched samples of PEDOT:PSS on PDMS continuously and noted the strain required to crack the films. The first crack appeared in a film at 12 ± 2% strain (N = 7), which corresponded to a frequency of ~0.05 cracks mm^{-1}. Subsequent strain produced additional stray cracks, but a significant frequency of cracks (~2 cracks mm^{-1}) did not appear until 30% strain. Increasing strain and cyclic loading of strain to a prescribed value produced new cracks—as opposed to widening existing ones. This observation supports the assertion that adhesion was strong enough to prevent significant delamination and global slipping of the PEDOT:PSS film. Interestingly, we also observed that topographic buckles in the PEDOT:PSS film left a permanent impression on the surface of the PDMS, when viewed after stripping off the PEDOT:PSS film with tape (see Supporting Information Figure S2). This observation suggests that the PDMS surface is deformed with the same frequency as the PEDOT:PSS layer, but the appearance of Figure 2c (top row of images) suggests that buckling occurred both with and without delamination.

To compare the electrical properties of PEDOT:PSS films on PDMS substrates activated using UV/O_3 and an oxygen plasma, we measured resistance while stretching the films up to 50% strain. Figure 3a plots the normalized resistance as a function of strain. Each plot represents 4−12 samples. The error bars represent the standard deviation. For clarity, we did not display error bars for the films supported by PDMS substrates treated for 180 s with plasma, but all such samples underwent large (>100×) increases in resistance between 5 and 10% strain. Films formed on PDMS treated with plasma for 10 s or UV/O_3 for 20 min did not undergo an abrupt increase in resistance. A comparison of the behavior of films on substrates treated for 10 s with plasma with and without Zonyl (Figure 3a, red vs blue curves) show that the presence of Zonyl decreases the effect of strain on resistance. The film with the smallest increase in resistance at the maximum strain tested was PEDOT:PSS coated from a solution containing 1% Zonyl on UV/O_3-treated PDMS (green). The resistance of the film increased by a factor of 2 at 50% strain. These data are replotted in Figure 3b, in which the y-axis is rescaled. The derivation of the plot labeled "hypothetical stretchable conductor" is discussed below.

Hypothetical Evolution of Resistance with Strain. The observed dependences of resistance on strain (the plots in Figure 2c) did not correspond to that of a hypothetical,

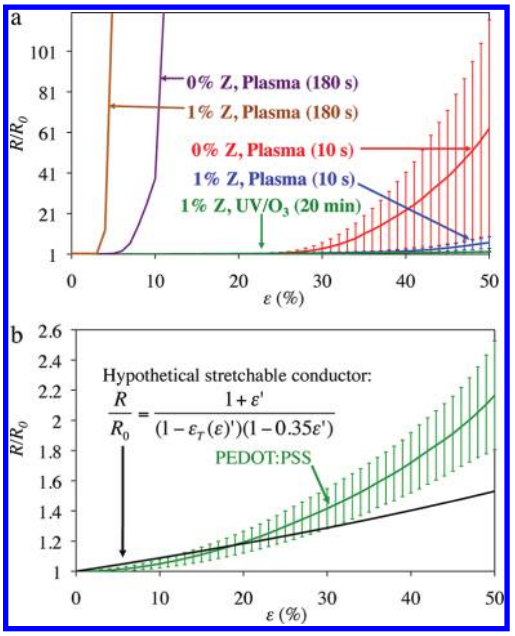

Figure 3. Effect of substrate activation on the evolution of resistance with strain for films of PEDOT:PSS. (a) Plots of normalized resistance vs strain for five combinations of methods of surface activation (an oxygen plasma for 180 or 10 s or UV/O_3 for 20 min) and addition of Zonyl ("Z") fluorosurfactant. The colors in which the data are rendered are consistent in all subsequent plots. (b) Plot of normalized resistance vs strain for the PEDOT:PSS film exhibiting the smallest increase in resistance with strain from (a). The axis has been rescaled. The plot for the hypothetical stretchable conductor is rendered in black.

homogeneous conductor that has no internal structure and does not crack when stretched. For an isotropic conductor (e.g., a metal), the resistance of a sample depends on its conductivity (σ) and geometry, as described by eq 2,

$$R = \frac{1}{\sigma}\frac{l}{wh} \tag{2}$$

where l, w, and h are the length, width, and height (thickness) of the sample. The dimensions of the sample change with strain, and the strain-dependent resistance of a film on an elastic substrate for small strains (ε < 10%) can be expressed by eq 3,

$$R(\varepsilon) = \frac{1}{\sigma}\frac{l(1+\varepsilon')}{w(1-\nu_s\varepsilon')h(1-\nu_f\varepsilon')} \tag{3}$$

where ν_s and ν_f are the Poisson ratio of the substrate and the film, and ε' is the fractional strain: $\varepsilon' = \varepsilon/100\%$. The term $(1+\varepsilon')$ accounts for the increase in length of the film when strained by ε'. The terms $(1-\nu_s\varepsilon')$ and $(1-\nu_f\varepsilon')$ account for the contraction in width and thickness with strain. We initially assumed that the Poisson ratio of the substrate constrained the decrease in width of the film, where ν_s = 0.5 for PDMS. The value of ν_s = 0.5 was too high for strains >10%, and we thus substituted the term $\nu_s\varepsilon'$ for an empirical function, $\varepsilon_T(\varepsilon)$, that describes the contraction in width (transverse strain) that we measured by hand, as a function of longitudinal strain (see Supporting Information Figure S3 for origin of $\varepsilon_T(\varepsilon)$).[18] We assumed the contraction of the thickness of the film was independent of the Poisson ratio of the PDMS substrate and used the value of ν_f = 0.35 for PEDOT:PSS.[18] We plotted the

dx.doi.org/10.1021/cm203216m | Chem. Mater. 2012, 24, 373−382

modified expression for $R(\varepsilon)$, divided by $R(0)$ (eq 4), on the same set of axes as the experimental data in Figure 3b.

$$\frac{R}{R_0} = \frac{1 + \varepsilon'}{(1 - \varepsilon_T(\varepsilon)')(1 - \nu_f\varepsilon')} \quad (4)$$

This plot represents the behavior of a hypothetical conductor undergoing the same geometric changes as did the PEDOT:PSS film. Interestingly, the experimental curve lies below the hypothetical curve for small strains (<18%); this behavior suggests that the conductivity of the PEDOT:PSS film increases with strain along the stretched axis.[39] For large strains, the normalized resistance of the PEDOT:PSS film was higher than that of the hypothetical stretchable conductor. We attribute this nonideal behavior to the accumulation of cracks in the PEDOT:PSS. We also plotted eq 4 for the extreme values of $\nu_f = 0$ and $\nu_f = 0.5$ in Supporting Information Figure S3, but our analysis is qualitatively similar within this range of values of ν_f (the quantitative difference is that the range of strain over which the experimental curve lies below the hypothetical curve decreases with ν_f from 0−24% using $\nu_f = 0.5$ to 0−10% using $\nu_f = 0$). To investigate the nanoscale morphological changes to films of PEDOT:PSS produced by strain, we obtained AFM images of the film when unstretched and stretched by 25% (Figure 4). When unstretched, the grains

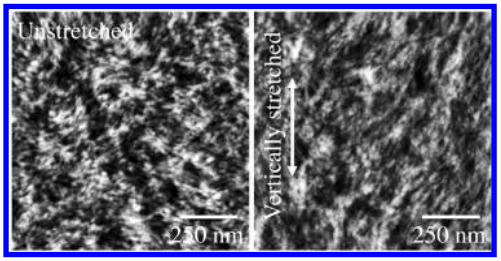

Figure 4. AFM height images of PEDOT:PSS films spin-coated from a solution containing 1% Zonyl on UV/O_3-treated PDMS. The unstretched film (left) exhibits grains with random orientations. When stretched by 25% (right), the grains appear to be aligned partially with the axis of strain.

in the film were randomly oriented. While stretched, the grains appeared to exhibit a slight preferential alignment along the axis of strain, which was also the direction of charge transport.

Strain-dependent conductivity has been observed in many polymeric, nanostructured, composite, and other anisotropic conductors. The enhancements of conductivity in stretch-aligned films of polyacetylene[44] and fibers of polyaniline are known phenomena.[45] Stretch-oriented films of P3HT exhibited an enhancement in field-effect mobility in the direction of stretching.[46] Hansen et al. observed enhancement of the conductivity in a composite elastomer of PEDOT and polyurethane.[39] We observed a similar effect in spray-deposited films of carbon nanotubes.[47] In that system, we found that stretching elongated and aligned wave-like bundles of nanotubes along the axis of strain and charge transport without destroying the junctions between nanotubes.[47] The concept of bulk conductivity does not seem directly applicable to anisotropic, stretchable conductors. For such materials, the most useful figures of merit are the unstrained conductivity, the gauge factor ($\Delta R/\Delta\varepsilon$, which may have different values at small and large strains[6]), and the maximum range of strain in which the change in resistance is reversible. For applications sensitive to changes in geometry with strain, it is also helpful to know the Poisson ratio of the stretchable conductor.

Effect of Surface Treatments on the Roughness and Morphology of PDMS after Stretching. To examine the possibility that damage to the substrate during stretching influenced the evolution of resistance vs strain, we subjected bare PDMS to three different treatments: exposure to UV/O_3 for 20 min, immersion in 10% hydrochloric acid, and oxidation with an oxygen plasma (400 mtorr O_2, 150 W) for 3 min. We then subjected the PDMS substrates to 20% strain and immediate relaxation to 0%. Figure 5 shows atomic force

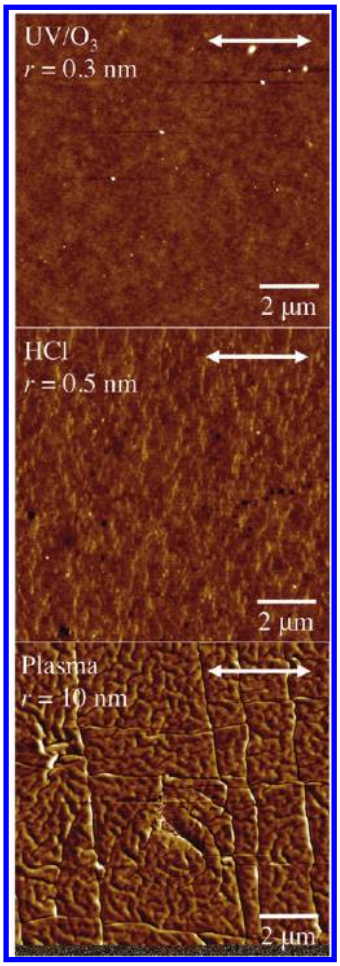

Figure 5. Change in morphology of PDMS substrates subjected to different methods of surface activation. Atomic force microscope (AFM) images of PDMS surfaces treated with UV/O_3 (top), hydrochloric acid (middle), and an oxygen plasma (bottom). All substrates were stretched to 20% and released before acquiring the images.

microscope (AFM) images of the three samples. Stretching did not produce features in the UV/O_3-treated substrates. The roughness (rms) of 0.3 nm was approximately that of the native surface of PDMS (before treatment). Treatment with hydrochloric acid and subsequent stretching produced a surface exhibiting fault-like features perpendicular to the axis of strain and increased roughness (0.5 nm). The surface of the plasma-treated PDMS exhibited extensive buckling perpendicular and parallel to the axis of strain and long cracks perpendicular to the axis of strain. The buckles and cracks produced a surface that was thus the roughest of those examined (10 nm). On the basis

dx.doi.org/10.1021/cm203216m | Chem. Mater. 2012, 24, 373−382

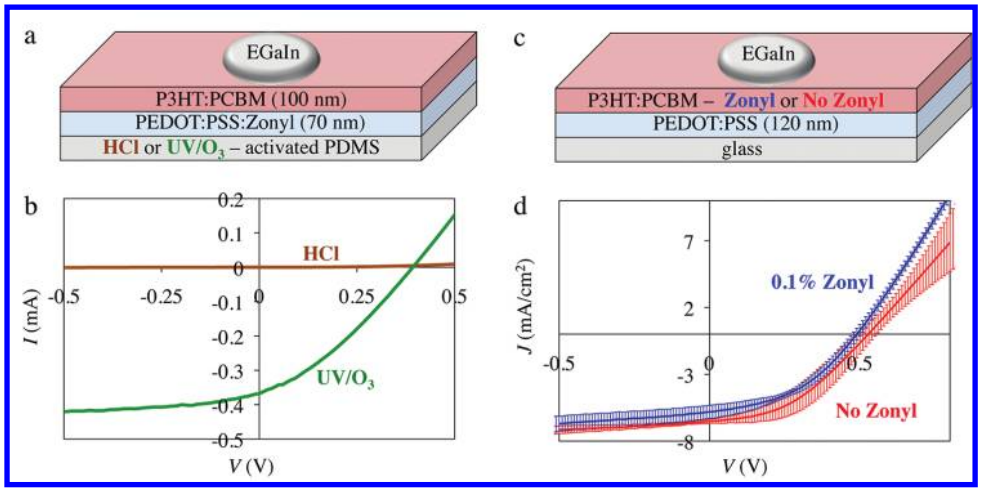

Figure 6. Effect of method of activation of the PDMS surface on photovoltaic properties of organic solar cells. (a) Schematic diagram of a bulk heterojunction organic photovoltaic device fabricated on PDMS substrate whose surface was activated using either hydrochloric acid (HCl) or UV/O_3. (b) Typical plots of current vs voltage for devices under illumination. The presence of trace HCl from the PDMS substrate had a deleterious effect on the photovoltaic properties of the device. In this pilot experiment, the efficiency of the device whose substrate was treated with UV/O_3 exhibited a power conversion efficiency of ~1%. (c) Schematic diagram of organic solar cells with or without deliberate contamination of the P3HT:PCBM active layer with Zonyl fluorosurfactant. (d) Plots of current density vs voltage for the device in which the active layer was contaminated with Zonyl (blue) and a control device, in which no Zonyl was present in any layer (red). The error bars represent the standard deviation of four and six devices (blue and red curves, respectively).

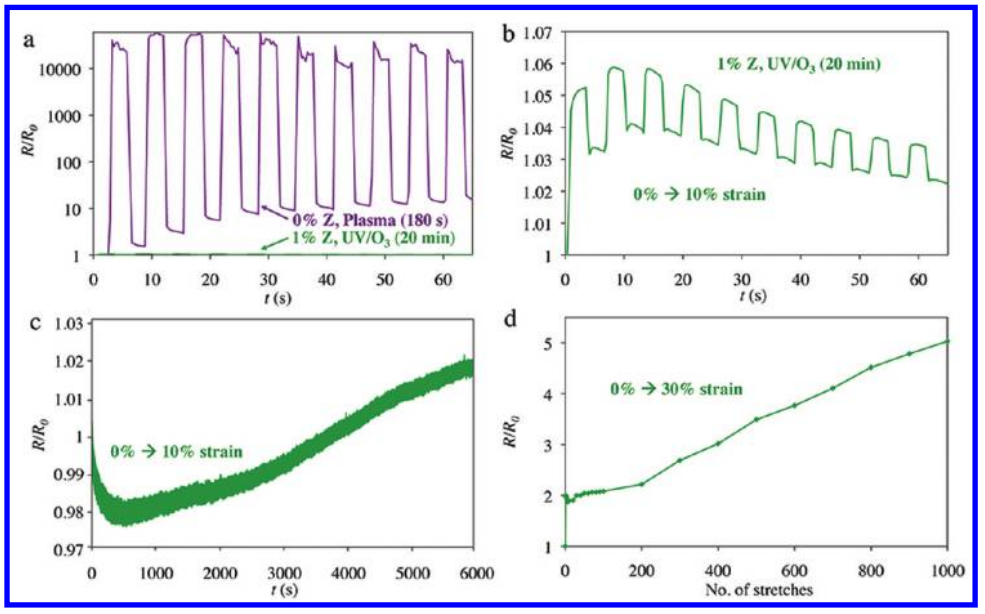

Figure 7. Evolution of resistance with cyclic loading of strain. (a) Plots of normalized resistance vs time over 10 cycles of applied strain to 10%. Note the *y*-axis is a log scale. The method of surface treatment had a dramatic effect on the change in resistance with stain. Plot (b) depicts the sample shown in green in plot (a), but the *y*-axis is rescaled. Plot (c) shows the evolution of resistance of the film over 1000 cycles of stretching from 0% to 10% strain. The net increase in resistance is ~2%. (d) Normalized resistance vs number of stretches for a film stretched from 0% to 30% strain. The resistance increases by a factor of 5 after 1000 stretches.

of these results, we reasoned that it was very likely that the change in the underlying morphology of the PDMS substrates upon stretching affected the electromechanical properties of thin films of PEDOT:PSS upon the application of strain.

Deleterious Effect of Trace Hydrochloric on Organic Solar Cells. While hydrolysis of the surface using hydrochloric acid is a common method of activating surfaces of PDMS,[18] we found that trace acid in the PDMS has a deleterious effect on the electronic properties of common organic semiconductors. Because our interest in mechanically compliant and fracture-resistant organic solar cells motivated our interest in the elasticity of PEDOT:PSS,[2,41] we fabricated bulk heterojunction photovoltaic devices on PDMS substrates (Figure 6a). We activated the PDMS with either hydrochloric acid or UV/O_3. The device employed a transparent electrode of PEDOT:PSS spin-coated from a solution with 1% Zonyl. The active layer was a 1:1 (by wt) blend of poly(3-hexylthiophene) (P3HT) and [6,6]-phenyl-C_{61}-butyric acid methyl ester (PCBM), and the top electrode was eutectic gallium–indium (EGaIn)[48]—a liquid metal compatible with stretchable electronic devices.[49] Figure 6b shows representative plots of current versus voltage. The devices on both the acid-treated ("HCl") and UV/O_3-

dx.doi.org/10.1021/cm203216m | *Chem. Mater.* 2012, 24, 373–382

treated substrates were measured under illumination with a solar simulator approximating the AM1.5G spectrum with a flux of 100 mW/cm^2. We found that the devices fabricated on hydrochloric acid-treated substrates had power conversion efficiencies of ≪0.1%, while those on UV/O_3-treated substrates had efficiencies of ∼1%. We tentatively attribute the deleterious effect of hydrochloric acid to partial degradation of the backbone of P3HT. We therefore abandoned the use of hydrochloric acid to activate PDMS substrates for stretchable organic electronic devices.

Effect of Contamination of Zonyl Fluorosurfactant in Organic Solar Cells. Concern that the Zonyl fluorosurfactant might diffuse from the PEDOT:PSS layer into or at the interface with the P3HT:PCBM active layer—as discussed by Norrman et al.[50]—led us to perform an experiment in which we added 0.1% Zonyl to the solution in 1,2-dichlorobenzene from which we spin-coated the bulk heterojunction. This intentional contamination represents what we believe would be an extreme case of the migration of Zonyl from the PEDOT:PSS to the P3HT:PCBM layers. Figure 6c describes the architectures of two devices fabricated on glass substrates: one in which the Zonyl was added to the P3HT:PCBM layer and a control device that did not contain Zonyl. Figure 6d shows plots of averaged current density (J) vs voltage for the two types of devices. The device in which the active layer was contaminated intentionally with Zonyl (N = 4, average power conversion efficiency = 1.2%) was 15% less efficient than the control device (N = 6, average power conversion efficiency 1.4%). The presence of Zonyl in the active layer produced a microscopically phase-separated morphology (see Supporting Information) that decreased—but did not destroy—the photovoltaic figures of merit.

Cyclic Loading and Fatigue Testing of Stretchable PEDOT:PSS Films. We subjected the films of PEDOT:PSS on plasma-treated and UV/O_3-treated PDMS substrates to cyclic applications of strain. Figure 7c plots the log of the normalized resistance versus time for 10 cycles of 0% to 10% strain. Whereas the resistance of the PEDOT:PSS film on plasma-treated PDMS increased by a factor of 10 000, the resistance of the film on the UV/O_3-treated substrate increased by <5% after 10 cycles. The drastically different relationship between resistance and strain for the films on two types of surfaces suggests different potential applications. For example, PEDOT:PSS films spin-coated from solutions containing Zonyl on UV/O_3-treated substrates could be used for transparent electrodes and interconnects in stretchable thin-film devices in which the resistance of the conductor should change minimally with strain,[15] while films of plasma-treated substrates could be used for strain sensors, where a high ratio of $\Delta R/\Delta\varepsilon$ ("gauge factor") is desirable.[51]

We performed fatigue testing on the PEDOT:PSS films containing Zonyl on UV/O_3-treated PDMS. In the first experiment, we subjected the film to 1000 cycles of stretching to 10% strain (Figure 7c). The film exhibited a decrease in resistance, which occurred around 100 cycles of strain, followed by an approximately linear increase in resistance thereafter. The net increase in resistance after 1000 cycles of strain was ∼2%. When we stretched a second film from 0% to 20% (also 1000 times), the net increase in resistance was 90%. Figure 7d shows the normalized resistance vs the number of stretches for a film stretched from 0% to 30%. The film underwent a fivefold (400%) increase in resistance after 1000 cycles, although the first stretch produced the first doubling of resistance.

Explanation of Reversible Stretchability for PEDOT:PSS on Plasma-Treated PDMS. To explain the large increase in resistance observed for PEDOT:PSS on PDMS treated with an oxygen plasma (Figure 7a, purple plot), we propose the model shown schematically in Figure 8. An oxygen plasma formed a brittle, silica-like (SiO_x) surface[52] on PDMS to which the PEDOT:PSS film strongly adhered. When the substrate was strained, the brittle surface of the PDMS fractured. Local strains in the PEDOT:PSS film at the sites of the cracks were significantly greater than the strain applied to the whole sample. These local strains were sufficient to fracture the PEDOT:PSS film and are consistent with the sharp increase in resistance measured at <10% strain, while no such abrupt increase in resistance occurred in films coated on UV/O_3-treated PDMS. Our electrical measurements were consistent

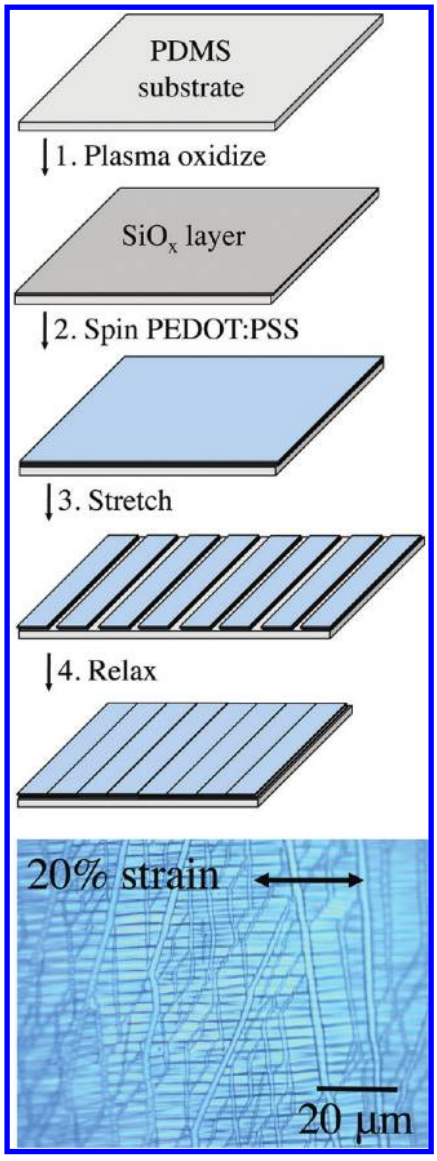

Figure 8. Proposed mechanism of reversible stretchability of films of PEDOT:PSS on plasma-treated PDMS. The plasma-treated PDMS bears a brittle layer of SiO_x, which dominates the electromechanical behavior of the PEDOT:PSS film. As the substrate is strained <10%, the brittle SiO_x layer fractures and causes the PEDOT:PSS film to fragment. The micrograph is a fractured PEDOT:PSS film on a plasma-treated PDMS substrate under 20% strain.

with the explanation that the electrical contiguity of the film was mostly destroyed upon stretching and restored upon relaxation for PEDOT:PSS films on plasma-treated substrates (as in Figure 3a, brown and purple curves, and Figure 7a, purple curve). The formation of percolated pathways between fractured plates of a thin film under strain is somewhat similar to the mechanism Graz et al. proposed for intentionally fractured films of gold on PDMS substrates.[21] Hansen et al. observed a similar effect in the fracturing of PEDOT–polyurethane elastomers on polyurethane substrates.[38] In the present work, however, the brittle surface of PDMS formed by plasma oxidation—as opposed to the intrinsic brittleness of PEDOT:PSS—dominated the fracturing of the film. For gold films subjected to >100 000 cycles of 0% to 20% strain, Graz et al. observed that percolated pathways were maintained in the stretched state because of out-of-plane bending and twisting of thin gold ligaments that maintained the electrical contiguity of the film.[21] The resistance of these gold films at 20% strain was thus only 3.5 times higher in the stretched state than in the unstretched state.[21] For PEDOT:PSS films on plasma-treated PDMS substrates, we do not believe there was a significant contribution to conductivity due to ligaments, because the conductivity in the stretched state was very poor ($\sim 10^{-2}$ S cm^{-1}).

Fabrication of Transparent Pressure Sensors. As a demonstration of the utility of these mechanically compliant, transparent thin films, we used them as electrodes in transparent, compressible pressure sensors[53] for interactive optoelectronic devices and other potential applications.[47] We fabricated the devices by cutting ~3-mm-wide strips in PDMS substrates bearing PEDOT:PSS films (Figure 9a). We positioned two strips face-to-face and offset by 90° and bonded them together using a thin layer of Ecoflex silicone elastomer (~300 μm). The Ecoflex served as both the bonding agent and the compressible dielectric layer in the capacitor.

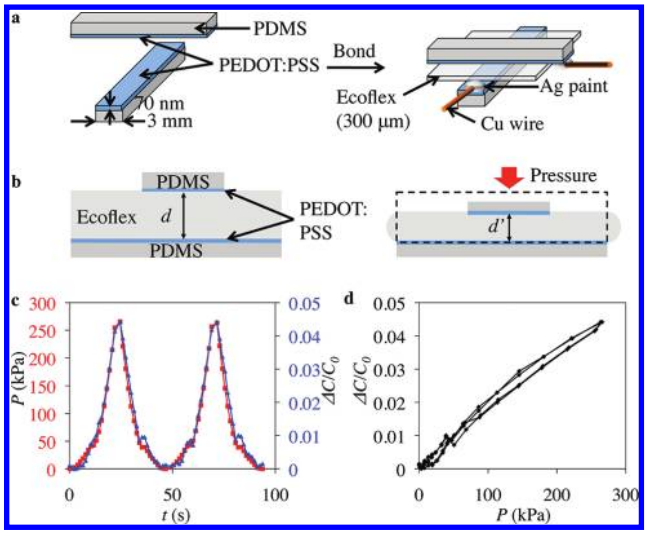

Figure 9. Schematic drawings and electrical characteristics of transparent, compressible pressure sensors comprising silicone elastomers and PEDOT:PSS electrodes. (a) Summary of the process used to fabricate devices. PDMS membranes supporting PEDOT:PSS films were cut into strips of ~3-mm width. These strips were bonded together using Ecoflex silicone elastomer. The termini of the PEDOT:PSS films were addressed using silver paint and copper wires. (b) Cross section of the region of overlap between the two strips. The thickness of the dielectric layer, d, decreases upon the application of pressure, d'. (c) Overlayed plots of pressure P and normalized change in capacitance $\Delta C/C_0$ capacitance vs time t over two cycles of applied pressure. (d) The same data shown in (c), but plotted as $\Delta C/C_0$ vs P.

The capacitance of a parallel plate capacitor is proportional to $1/d$, where d is the distance between parallel plates. Applying pressure to a parallel plate capacitor comprising a compressible dielectric layer shortens d (to d', Figure 9b). The decreased spacing between the electrodes manifests as an increase in capacitance. We carried out the measurements of capacitance vs pressure by placing the device on a vertically translatable stage. The stage pushed the device into a fixed force gauge. In order to prevent electronic interference from the metallic probe of the force gauge, we placed ~2 mm^2 glass squares between the device and the probe. The glass square defined the area of contact that we used to calculate pressure from force. In future applications, it will be necessary to fabricate an internal shielding mechanism to prevent external conductors (e.g., human skin) from changing the capacitance by fringe-field effects.[7] Figure 9c shows a plot of applied pressure overlaid with the normalized change in capacitance $\Delta C/C_0$ as a function of time. The change in capacitance closely followed the applied pressure but deviated when the device was unloaded. This hysteretic behavior can be seen more clearly in Figure 9d, which plots normalized change in capacitance vs pressure. A contributing factor to the hysteresis could be the viscoelasticity of the PDMS, the Ecoflex, or the PEDOT:PSS.[53] The use of UV/O_3 to activate the surfaces of PDMS was critical to produce working devices. When we activated the surfaces using an oxygen plasma, we observed irreversible changes in capacitance and could not fabricate a functional device. It is likely that the strains produced by compression of the device were sufficient to crack the silica-like skin of the surface of plasma-treated PDMS.

CONCLUSION

There are five key findings of this study. (i) PEDOT:PSS films containing Zonyl fluorosurfactant on UV/O_3-activated PDMS substrates are stretchable and retain substantial conductivity up to 188% strain. The dependence of resistance on strain exhibits some reversibility up to 30% strain. (ii) The method used to activate the PDMS substrate has a dramatic effect on the dependence of resistance on strain for PEDOT:PSS films. For PEDOT:PSS films on PDMS substrates activated by an oxygen plasma, the brittle silica-like skin causes the PEDOT:PSS overlayer to fracture at strains <10%. (iii) For PEDOT:PSS films containing Zonyl and coated on UV/O_3-activated PDMS, AFM images of stretched films suggest that the PEDOT:PSS grains reorient in the direction of the strain and accommodate tensile deformation. (iv) The tensile deformation of PEDOT:PSS films was plastic and produced buckled films after the initial stretch. These buckles—as opposed to intrinsic elasticity of the film—accommodated additional cycles of stretching. (v) The ability to withstand tensile deformation allows PEDOT:PSS containing Zonyl to be used in applications requiring tensile deformation, such as the transparent electrode materials for transparent, compressible pressure sensors.

Our observations that the resistance of PEDOT:PSS containing Zonyl on UV/O_3-treated PDMS substrates was lower than the resistance of a hypothetical isotropic conductor (e.g., a metal) for modest strains (e.g., <18%) is interesting. The implication is that the conductivity of PEDOT:PSS increases with strain in a way that partially offsets the effects

dx.doi.org/10.1021/cm203216m | Chem. Mater. 2012, 24, 373–382

of lengthening of the sample and concomitant reduction in cross sectional area. We suggest that the effective increase in conductivity with strain (albeit small strains in the case of PEDOT:PSS) is an instance of a general phenomenon observed in conductive polymers, nanostructured thin films, and other anisotropic, stretchable conductors in which it is possible to align the current-carrying components with the axis of strain. It might even be possible to design a planar (e.g., not buckled) material that experiences no increase in resistance at high strains.

The use of three commercial materials—PEDOT:PSS, Zonyl, and PDMS—to form stretchable conductors has immediate implications for electronic devices requiring transparency, extreme flexibility, and stretchability. PEDOT:PSS, cast into thin films as described in this paper, has a very favorable combination of transparency, elasticity, and bulk conductivity and is simple to integrate into optoelectronic devices that have planar architectures, such as displays and solar cells.[2,41] Further, other materials[2] that are currently under investigation for "ITO-free"[54] optoelectronic devices cannot tolerate the level of strain we demonstrated for PEDOT:PSS on PDMS. The generation of stretchable conductors on unprestrained substrates using commercial, unmodified, and well-characterized materials, such as PEDOT:PSS and PDMS, substantially simplifies patterning and integration of device components for mechanically compliant electronics.

EXPERIMENTAL METHODS

Materials. We purchased the PEDOT:PSS solution (Clevios PH 1000) from Heraeus. The solid content was 1−1.3% and had a PEDOT to PSS ratio of 1:2.5 by weight. Zonyl FS-300 (Zonyl), *ortho*-dichlorobenzene (ODCB), poly(3-hexylthiophene) (P3HT, regioregular, >90% head-to-tail regiospecificity), [6,6]-phenyl C_{61} butyric acid methyl ester (PCBM, >99%), and eutectic gallium−indium (EGaIn, ≥99.99%) were purchased from Sigma-Aldrich and used as received. Dimethylsulfoxide (DMSO) was purchased from Acros and used as supplied. The PDMS was prepared by curing a mixed and degassed PDMS prepolymer (Dow Corning Sylgard 184, with a ratio of base to cross-linker of 10:1 by mass) against the polished surface of a silicon wafer. It was then cured at 60 °C for 2 h to produce PDMS substrates with thicknesses of ∼300 μm. The PDMS substrates were cut into 4 mm × 2 mm rectangles, which were placed with the flat side up on glass slides, which served as the supports for spin-coating and thermal annealing.

Preparation of PEDOT:PSS Solutions and Casting of Films. The PEDOT:PSS solution containing 5% DMSO was filtered through a syringe filter (1 μm pore size) to remove precipitated material. Where noted in the main text, 1% Zonyl by volume was added to the PEDOT:PSS. The solution was mixed with a vortex mixer for 20 s. We spin-coated the solutions (1 krpm for 60 s, then 2 krpm for 60 s, unless otherwise noted) on the flat surfaces of PDMS that received treatment with an oxygen plasma (150 W, 400 mtorr O_2, 10 or 180 s), hydrochloric acid (10% HCl in water, immersed for 16 h), or UV/O_3 (using a Jelight Model No. 42 UVO-Cleaner equipped with a low pressure mercury vapor grid lamp with an output of 28 mW/cm at 254 nm, with the substrate placed 6 mm from the light source, for 20 min). The films were placed on a hot plate in ambient air for 10 min (Figures 2a,b,d) or 30 min (all other samples) at 150 °C. The hot plate was turned off, and the films were allowed to cool for an additional 30 min. The dependence of normalized resistance on strain was not sensitive to the interval over which the film was heated, but the most conductive films (R_S = 260 Ω sq^{-1}) were heated for 10 min at 150 °C, followed by a 30-min cooling to ambient temperature.

Characterization of PEDOT:PSS Films. AFM images were taken using tapping mode (light tapping regime) using a Multimode AFM (Veeco). We measured sheet resistance using the four-point van der Pauw method with collinear probes (0.5 cm spacing) connected to a Keithley 2400 Sourcemeter. The dimensions of the samples were 5 mm × 20 mm. Optical micrographs of the films were taken using a Leica DM4000 M microscope under bright-field illumination. Optical transmission measurements were performed on Cary 6000i spectrophotometer from 250 to 1250 nm. Reported transmittances (T) are at 550 nm. Stretching cycles were performed on an in-house stretching station with films on the PDMS substrate cut to dimensions of 3 mm × 2.5 cm. EGaIn electrodes were used to make conformal contact with the PEDOT:PSS films while applying strain and were applied to the ends of the PEDOT:PSS films using a syringe. Copper wires were placed in the drops of EGaIn. The PEDOT:PSS films on the PDMS substrates, the EGaIn, and the copper wires were clamped to immobilize the termini of the samples while stretching. The copper wires were connected to an Agilent E4980A LCR meter to measure 2-point resistance during the stretching cycles.

Fabrication and Characterization of Organic Solar Cells. We spin-coated PEDOT:PSS films from solutions containing 1% Zonyl on PDMS substrates activated using either hydrochloric acid or UV/O_3. We prepared P3HT:PCBM films from a 1:1 (w/w) solution of 30 mg/mL total in ODCB. This solution was spin-coated at 700 rpm for 1 min and 2000 rpm for 1 min on the PEDOT:PSS/PDMS substrates. After spin coating, the substrates were transferred to a nitrogen glovebox and annealed on a hot plate at 150 °C for 30 min; after annealing, the hot plate was turned off and the substrate was allowed to cool gradually for 30 min. The substrates were then removed from the glovebox and EGaIn was deposited on top for the top electrode. Copper wires were placed in each drop of EGaIn and secured to the edge of the substrate with tape. The devices were immediately returned to the glovebox (total time in the ambient atmosphere was <10 min). Typical device areas were ∼0.05 cm^2. The photovoltaic properties were measured using a Newport solar simulator with a 100 mW/cm^2 flux that approximated the solar spectrum under AM 1.5G conditions. We measured the current density versus voltage in the dark and under illumination using a Keithley 2400 Sourcemeter and collected the data electronically using a custom LabView script. We used the same procedures for fabrication in the experiment in which we examined the effect of Zonyl contamination on the bulk heterojunction (Figure 6c,d), except that we used plasma-treated glass substrates instead of PDMS and we did not add Zonyl to the PEDOT:PSS solution. Instead, we added Zonyl to the P3HT:PCBM solution for one set of samples.

Fabrication and Characterization of Transparent, Compressible Pressure Sensors. We fabricated pressure sensors by gluing two PDMS substrates bearing PEDOT:PSS films face-to-face using Ecoflex silicone elastomer (Smooth-On 0010). Thermal curing (60 °C, 2 h) produced devices with compressible dielectric layers of loosely defined thickness, but 100−300 μm was typical. We connected copper wires to the termini of the PEDOT:PSS lines using silver paint as a conductive adhesive. We measured resistance and capacitance using an LCR meter (Agilent E498A precision LCR meter) interfaced with a custom LabView script. We measured capacitance versus pressure by applying compressive force perpendicular to the device by placing the device between a programmable vertically movable stage and a force gauge (Mark-10 model BG05) with a probe with an area of contact defined by a square cut from a glass slide.

ASSOCIATED CONTENT

Supporting Information

Optical micrographs of organic solar cells contaminated with Zonyl, evidence for permanent deformation of PDMS by buckled PEDOT:PSS, and a discussion of the contraction in width of PDMS membranes for strains >10%. This information is available free of charge via the Internet at http://pubs.acs.org.

AUTHOR INFORMATION

Corresponding Author

*E-mail: zbao@stanford.edu.

■ ACKNOWLEDGMENTS

D.J.L. was supported by a U.S. Intelligence Community Postdoctoral Fellowship. This work was partially supported by the Global Climate and Energy Project at Stanford University.

■ REFERENCES

(1) Rogers, J. A.; Someya, T.; Huang, Y. G. *Science* **2010**, *327*, 1603.
(2) Lipomi, D. J.; Bao, Z. N. *Energy Environ. Sci.* **2011**, *4*, 3314.
(3) Kaltenbrunner, M.; Kettlgruber, G.; Siket, C.; Schwodiauer, R.; Bauer, S. *Adv. Mater.* **2010**, *22*, 2065.
(4) Viventi, J.; Kim, D. H.; Moss, J. D.; Kim, Y. S.; Blanco, J. A.; Annetta, N.; Hicks, A.; Xiao, J. L.; Huang, Y. G.; Callans, D. J.; Rogers, J. A.; Litt, B. *Sci. Transl. Med.* **2010**, *2*, 24ra22.
(5) Someya, T. *Nat. Mater.* **2010**, *9*, 879.
(6) Yamada, T.; Hayamizu, Y.; Yamamoto, Y.; Yomogida, Y.; Izadi-Jajafabadi, A.; Futaba, D. N.; Hata, K. *Nat. Nanotechnol.* **2011**, *6*, 296.
(7) Cotton, D. P. J; Graz, I. M.; Lacour, S. P. *IEEE Sens. J.* **2009**, *9*, 2008.
(8) Krebs, F. C.; Nielsen, T. D.; Fyenbo, J.; Wadstrom, M.; Pedersen, M. S. *Energy Environ. Sci.* **2010**, *3*, 512.
(9) Wu, H.; Hu, L. B.; Rowell, M. W.; Kong, D. S.; Cha, J. J.; McDonough, J. R.; Zhu, J.; Yang, Y. A.; McGehee, M. D.; Cui, Y. *Nano Lett.* **2010**, *10*, 4242.
(10) Vosgueritchian, M.; Lipomi, D. J.; Bao, Z. N. *Adv. Funct. Mater.* **2011**, DOI: 10.1002/adfm.201101775.
(11) Kim, D. H.; Xiao, J. L.; Song, J. Z.; Huang, Y. G.; Rogers, J. A. *Adv. Mater.* **2010**, *22*, 2108.
(12) Krebs, F. C.; Tromholt, T.; Jorgensen, M. *Nanoscale* **2010**, *2*, 873.
(13) Sekitani, T.; Someya, T. *Adv. Mater.* **2010**, *22*, 2228.
(14) Sekitani, T.; Nakajima, H.; Maeda, H.; Fukushima, T.; Aida, T.; Hata, K.; Someya, T. *Nat. Mater.* **2009**, *8*, 494.
(15) Sekitani, T.; Noguchi, Y.; Hata, K.; Fukushima, T.; Aida, T.; Someya, T. *Science* **2008**, *321*, 1468.
(16) Baca, A. J.; Ahn, J. H.; Sun, Y. G.; Meitl, M. A.; Menard, E.; Kim, H. S.; Choi, W. M.; Kim, D. H.; Huang, Y.; Rogers, J. A. *Angew. Chem., Int. Ed.* **2008**, *47*, 5524.
(17) O'Connor, B.; Chan, E. P.; Chan, C.; Conrad, B. R.; Richter, L. J.; Kline, R. J.; Heeney, M.; McCulloch, I.; Soles, C. L.; DeLongchamp, D. M. *ACS Nano* **2010**, *4*, 7538.
(18) Tahk, D.; Lee, H. H.; Khang, D. Y. *Macromolecules* **2009**, *42*, 7079.
(19) Chun, K. Y.; Oh, Y.; Rho, J.; Ahn, J. H.; Kim, Y. J.; Choi, H. R.; Baik, S. *Nat. Nanotechnol.* **2010**, *5*, 853.
(20) Lacour, S. P.; Chan, D.; Wagner, S.; Li, T.; Suo, Z. *Appl. Phys. Lett.* **2006**, *88*, 204103.
(21) Graz, I. M.; Cotton, D. P. J; Lacour, S. P. *Appl. Phys. Lett.* **2009**, *98*, 071902.
(22) Stec, H. M.; Williams, R. J.; Jones, T. S.; Hatton, R. A. *Adv. Funct. Mater.* **2011**, *21*, 1709.
(23) Rathmell, A. R.; Bergin, S. M.; Hua, Y. L.; Li, Z. Y.; Wiley, B. J. *Adv. Mater.* **2010**, *22*, 3558.
(24) Hu, L. B.; Kim, H. S.; Lee, J. Y.; Peumans, P.; Cui, Y. *ACS Nano* **2010**, *4*, 2955.
(25) Suo, Z.; Ma, E. Y.; Gleskova, H.; Wagner, S. *Appl. Phys. Lett.* **1999**, *74*, 1177.
(26) Yu, C. J.; Masarapu, C.; Rong, J. P.; Wei, B. Q.; Jiang, H. Q. *Adv. Mater.* **2009**, *21*, 4793.
(27) Bae, S.; Kim, H.; Lee, Y.; Xu, X. F.; Park, J. S.; Zheng, Y.; Balakrishnan, J.; Lei, T.; Kim, H. R.; Song, Y. I.; Kim, Y. J.; Kim, K. S.; Ozyilmaz, B.; Ahn, J. H.; Hong, B. H.; Iijima, S. *Nat. Nanotechnol.* **2010**, *5*, 574.
(28) Rowell, M. W.; McGehee, M. D. *Energ. Environ. Sci.* **2011**, *4*, 131.
(29) Yu, Z. B.; Niu, X. F.; Liu, Z.; Pei, Q. B. *Adv. Mater.* **2011**, *23*, 3989.
(30) Elschner, A.; Kirchmeyer, S.; Lovenich, W.; Merker, U.; Reuter, K. *PEDOT: Principles and Applications of an Intrinsically Conductive Polymer*; CRC: New York, 2011.
(31) Crispin, X.; Jakobsson, F. L. E.; Crispin, A.; Grim, P. C. M.; Andersson, P.; Volodin, A.; van Haesendonck, C.; Van der Auweraer, M.; Salaneck, W. R.; Berggren, M. *Chem. Mater.* **2006**, *18*, 4354.
(32) Kim, Y. H.; Sachse, C.; Machala, M. L.; May, C.; Muller-Meskamp, L.; Leo, K. *Adv. Funct. Mater.* **2011**, *21*, 1076.
(33) Hau, S. K.; Yip, H. L.; Zou, J. Y.; Jen, A. K. Y. *Org. Electron.* **2009**, *10*, 1401.
(34) Stafford, C. M.; Harrison, C.; Beers, K. L.; Karim, A.; Amis, E. J.; Vanlandingham, M. R.; Kim, H. C.; Volksen, W.; Miller, R. D.; Simonyi, E. E. *Nat. Mater.* **2004**, *3*, 545.
(35) Invernale, M. A.; Ding, Y.; Sotzing, G. A. *ACS Appl. Mater. Interfaces* **2010**, *2*, 296.
(36) Ding, Y.; Invernale, M. A.; Sotzing, G. A. *ACS Appl. Mater. Interfaces* **2010**, *2*, 1588.
(37) Blau, A.; Murr, A.; Wolff, S.; Sernagor, E.; Medini, P.; Iurilli, G.; Ziegler, C.; Benfenati, F. *Biomaterials* **2011**, *32*, 1778.
(38) Hansen, T. S.; Hassager, O.; Larsen, N. B.; Clark, N. B. *Synth. Met.* **2007**, *157*, 961.
(39) Hansen, T. S.; West, K.; Hassager, O.; Larsen, N. B. *Adv. Funct. Mater.* **2007**, *17*, 3069.
(40) Kwon, S. J.; Kim, T. Y.; Lee, B. S.; Lee, T. H.; Kim, J. E.; Suh, K. S. *Synth. Met.* **2010**, *160*, 1092.
(41) Lipomi, D. J.; Tee, B. C.-K.; Vosgueritchian, M.; Bao, Z. N. *Adv. Mater.* **2011**, *23*, 1771.
(42) Sekitani, T.; Zschieschang, U.; Klauk, H.; Someya, T. *Nat. Mater.* **2010**, *9*, 1015.
(43) Voigt, M. M.; Mackenzie, R. C. I.; Yau, C. P.; Atienzar, P.; Dane, J.; Keivanidis, P. E.; Bradley, D. D. C.; Nelson, J. *Sol. Energy Mater. Sol. Cells* **2011**, *95*, 731.
(44) Cao, Y.; Smith, P. A.; Heeger, A. J. *Synth. Met.* **1991**, *41*−*43*, 181.
(45) Pomfret, S. J.; Adams, P. N.; Comfort, N. P.; Monkman, A. P. *Polymer* **2000**, *41*, 2265.
(46) Yasuda, T.; Han, L. Y.; Tsutsui, T. *J. Photopolym. Sci. Technol.* **2009**, *22*, 713.
(47) Lipomi, D. J.; Vosgueritchian, M.; Tee, B. C.-K.; Fox, C. H.; Lee, J. A.; Bao, Z. N. *Nat. Nanotechnol.* **2011**, *6*, 788.
(48) Chiechi, R. C.; Weiss, E. A.; Dickey, M. D.; Whitesides, G. M. *Angew. Chem., Int. Ed.* **2008**, *47*, 142.
(49) So, J. H.; Thelen, J.; Qusba, A.; Hayes, G. J.; Lazzi, G.; Dickey, M. D. *Adv. Funct. Mater.* **2009**, *19*, 3632.
(50) Norrman, K.; Madsen, M. V.; Gevorgyan, S. A.; Krebs, F. C. *J. Am. Chem. Soc.* **2010**, *132*, 16883.
(51) Cao, Q.; Rogers, J. A. *Adv. Mater.* **2009**, *21*, 29.
(52) Hillborg, H.; Ankner, J. F.; Gedde, U. W.; Smith, G. D.; Yasuda, H. K.; Wikström, K. *Polymer* **2000**, *41*, 6851.
(53) Mannsfeld, S. C. B.; Tee, B. C. K.; Stoltenberg, R. M.; Chen, C. V. H. H.; Barman, S.; Muir, B. V. O.; Sokolov, A. N.; Reese, C.; Bao, Z. N. *Nat. Mater.* **2010**, *9*, 859.
(54) Manceau, M.; Angmo, D.; Jorgensen, M.; Krebs, F. C. *Org. Electron.* **2011**, *12*, 566.